Available online at www.sciencedirect.com
SCIENCE DIRECT®
ELSEVIER
Bioorganic & Medicinal Chemistry Letters 16 (2006) 1679–1685
Bioorganic & Medicinal Chemistry Letters

# Discovery of *trans*-3,4′-bispyridinylethylenes as potent and novel inhibitors of protein kinase B (PKB/Akt) for the treatment of cancer: Synthesis and biological evaluation

Qun Li,[a,*] Tongmei Li,[a] Gui-Dong Zhu,[a] Jianchun Gong,[a] Akiyo Claibone,[a] Chris Dalton,[a] Yan Luo,[a] Eric F. Johnson,[a] Yan Shi,[a] Xuesong Liu,[a] Vered Klinghofer,[a] Joy L. Bauch,[a] Kennan C. Marsh,[a] Jennifer J. Bouska,[a] Shannon Arries,[a] Ron De Jong,[b] Tilman Oltersdorf,[b] Vincent S. Stoll,[a] Clarissa G. Jakob,[a] Saul H. Rosenberg[a] and Vincent L. Giranda[a]

[a]*Cancer Research, GPRD, Abbott Laboratories, Abbott Park, IL 60064-6101, USA*
[b]*Idun Pharmaceuticals, 9380 Judicial Dr., San Diego, CA 92121, USA*

Received 10 November 2005; revised 1 December 2005; accepted 2 December 2005
Available online 5 January 2006

**Abstract**—A novel series of Akt/PKB inhibitors derived from a screening lead (**1**) has been prepared. The novel *trans*-3,4′-bispyridinylethylenes described herein are potent inhibitors of Akt/PKB with $IC_{50}$ values in the low double-digit nanomolar range against Akt1. Compound **2q** shows excellent selectivity against distinct families of kinases such as tyrosine kinases and CAMK, and displays poor to modest selectivity against closely related kinases in the AGC and CMGC families. The cellular activities including inhibition of cell growth and phosphorylation of downstream target GSK3 are also described. The X-ray structure of compound **2q** complexed with PKA in the ATP binding site was determined.


Akt inhibitors[1] have recently generated much attention as anticancer agents because of their role of intervention in a signal transduction pathway crucial for proliferation and survival of cancer cells.[2] Akt, also known as protein kinase B (PKB), is a serine/threonine kinase that belongs to the AGC family of kinases.[3] There exist three human isoforms of Akt: Akt1, Akt2, and Akt3. These isoforms have a high degree of overall homology being about 80% identical. They share similar downstream targets, but differ in levels of expression and activation in response to stimuli in various tumors.[2e]

Akt is one of the major direct downstream targets of class I PI3K. When activated in response to extracellular stimulation, PI3K phosphorylates glycerophospholipid PtdIns(4, 5)P2, leading to rapid production of PtdIns(3, 4, 5)P3 in the cell membrane, which in turn recruits Akt from the cytoplasm to the membrane by binding to the PH domain of Akt. This binding induces conformational changes in Akt, exposing its main phosphorylation sites and bringing it in proximity with PDK1 thereby enabling phosphorylation at Thr308 by PDK1. The additional phosphorylation at Ser473 of the C-terminus is carried out by putative PDK2. This is thought to stabilize the active conformation of the kinase domain, leading to fully activated Akt that dissociates from the membrane. It then enters the cytoplasm and nucleus where its substrates are located. So far about 20 Akt substrates have been identified.[2e]

Compelling evidence supports the importance of Akt in inducing tumorigenicity both in vitro and in vivo.[2] Akt is overexpressed and constitutively active in a large number of human tumors. Akt antisense oligonucleotides were found to inhibit proliferation and induce apoptosis in several cancer cell lines. A recent study has shown that inhibition of Akt via antisense RNA reduced Akt expression in pancreatic tumorigenicity and invasiveness in nude mice.[4]

*Keywords*: Akt inhibitors; Akt; PKB; Protein kinase B; GSK3; FL5.12-Akt1; Anticancer; Apoptosis; X-ray.
* Corresponding author. Tel.: +1 847 937 7125; fax: +1 847 936 1550; e-mail: qun.li@abbott.com

0960-894X/$ - see front matter © 2005 Elsevier Ltd. All rights reserved.
doi:10.1016/j.bmcl.2005.12.017

Compound **1** was identified as a promising Akt inhibitor lead from our compound library. It is an ATP competitive inhibitor with an $IC_{50}$ of 5.29 μM against Akt1. We report herein the structure refinements of **1** that produced a novel and potent series of *trans*-3,4′-bispyridinylethylenes as Akt inhibitors represented by **2q** (Fig. 1).

Synthesis of the *trans*-ethylene analogs of our lead (**2**, **5**, **6**, **7**, and **10**) is illustrated in Scheme 1. Mitsunobu reaction of hydroxybromide **3** with the corresponding alcohol provided ether **4**, which in turn was converted to alkenes **2**, **5**, or **6** by the Heck reaction followed by deprotection of the Boc group with TFA. Acetyloxy-de-diazonization of **2q** followed by hydrolysis produced hydroxyl analog **7a**. The 2-substituted pyridine analogs (**10**) were prepared from 2-fluoro-4-vinylpyridine **9** using the Heck reaction–alkylation sequence followed by Boc deprotection.

Preparation of analogs with the side chains attached to the central pyridine through carbon (**15**) or nitrogen (**16** and **17**) is shown in Scheme 2. 3-Amino-5-bromopyridine **11** underwent the Heck reaction with 4-vinylpyridine, followed by the iodo-de-diazonization

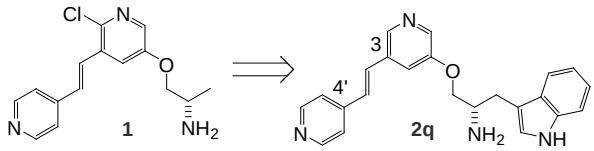


**Figure 1.** Modifications of a high throughput lead (**1**) resulted in potent Akt inhibitor **2**.

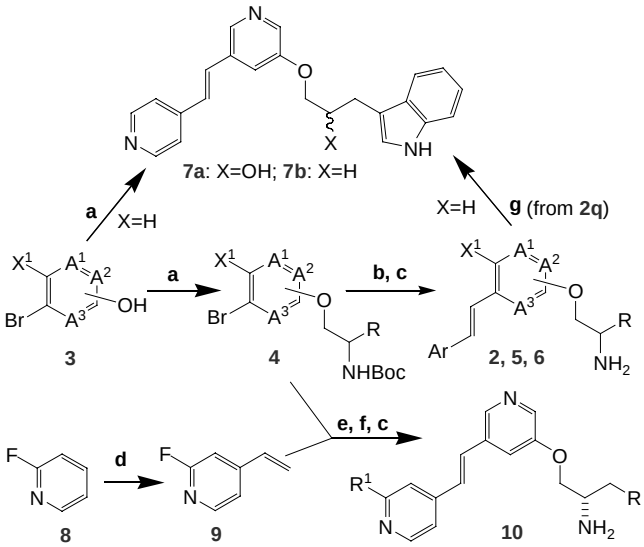


**Scheme 1.** Reagents and conditions: (a) Substituted 2-Boc-aminoethanol, DEAD/$PPh_3$, THF, rt, 50–90%; (b) ArCH=$CH_2$, P(*o*-Tol)$_3$, Pd(OAc)$_2$, $CH_3CN$, 80 °C, 8 h, 40–73%; (c) TFA, $CH_2Cl_2$, rt, 2 h; (d) i—LDA, THF, −78 °C, 30 min, $I_2$, 30 min, 88%; ii—LDA, THF, −78 °C, 30 min, 81%;[5] iii—$SnBu_3$=$CH_2$, $Pd_2Cl_2(PPh_3)_2$, dioxane, 80 °C, overnight, 38%; (e) P(*o*-Tol)$_3$, Pd(Ac)$_2$, $CH_3CN$, 80 °C, 8 h, 84%; (f) NaOMe, MeOH, reflux, 8 h, 75%, or PhOH or RSH, KOH, 140 °C, 5–60%, or $RNH_2$, DMF, 125 °C, 1.5–36 h, 3–60%; (g) i—$NaNO_2$, AcOH, rt, 18 h, 12%; ii—LiOH, water/THF, 55 °C, overnight, 57%.

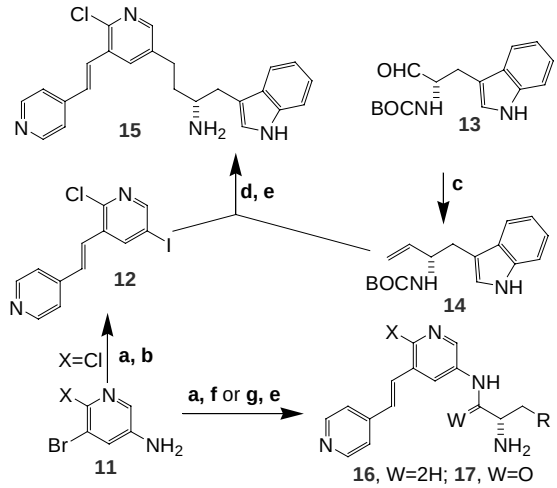


**Scheme 2.** Reagents and conditions: (a) 4-vinylpyridine, $Pd_2(dba)_3$, P(*o*-Tol)$_3$, $Et_3N$, DMF, 100 °C, 15 h, 36–84%; (b) $NaNO_2$, 30% $H_2SO_4$, 0 °C, 5 h, then NaI, 2 h, 70%; (c) $Ph_3PCH_3Br$, *n*-BuLi, THF, 0 °C, 30 min, then **13**, 2 h, 18%; (d) **14**, 9-BBN, 0 °C to rt, overnight, then **12**, $PdCl_2$(dppf), $Cs_2CO_3$, DMF, 50 °C, 8 h, 40%; (e) TFA, $CH_2Cl_2$, rt, 2 h, 74–100%; (f) **9**, AcOH, MeOH, reflux, 3 h, then $NaBH_3CN$, 1 h, 35–70%; (g) α-Boc-amino acid, EDC/HOBt/DMAP, THF, overnight, 41–55%.

resulting in iodopyridine **12**. The latter was reacted with ethylene **14** in the presence of 9-BBN and $PdCl_2$(dppf) to give compound **15**. Reductive amination of **11** with *N*-Boc-tryptophanal by $NaBH_3CN$ in the presence of Ti(*i*-PrO)$_4$ and subsequent acidic deprotection of the Boc group provided benzylamine **16**. Aminopyridine **11** was converted to amides **17** through EDC coupling reactions with Boc-protected amino acids followed by deprotection with TFA.

Compounds **22a** and **b**, in which an aryl side chain is attached to the β-position of the primary amine, were synthesized as shown in Scheme 3. Nucleophilic substitution of 3,5-dibromopyridine with the acetonitrile anions yielded **19**, which after reduction to amine **20** with borane followed by Boc protection afforded **21**. Heck reaction and subsequent acidic deprotection as described previously provided **22**.

Our initial optimization efforts focused on modifications of the amino acid-derived side chain of lead compound **1**

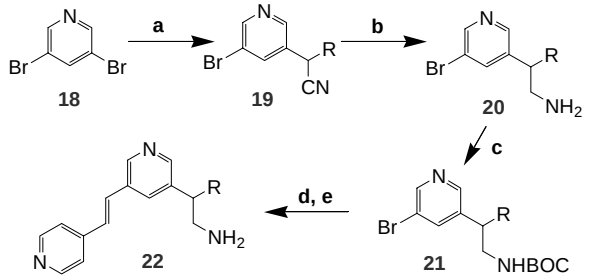


**Scheme 3.** Reagents and conditions: (a) $RCH_2CN$, NaH, DMF, rt, 2 h, 33–99%; (b) $BH_3$·THF, THF, rt, overnight, 73–84%; (c) $(BOC)_2O$, $CH_3CN$, rt, overnight, 78–98%; (d) 4-vinylpyridine, P(*o*-Tol)$_3$, Pd(Ac)$_2$, $CH_3CN$, 80 °C, 8 h; (e) TFA, $CH_2Cl_2$, rt, 2 h, 23–27% for two steps.

**Table 1.** Activity of Akt inhibitors[a]

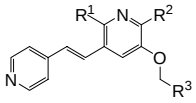

| Compound | $R^1$ | $R^2$ | $R^3$ | Akt1 $IC_{50}$[a] (nM) |
|---|---|---|---|---|
| **1** (lead) | Cl | H |  | 5290 |
| **2a** | H | H |  | 5080 |
| **2b** | H | H |  | 14,710 |
| **2c** | H | H |  | 19,320 |
| **2d** | H | H |  | 11%[b] |
| **2e** | H | H |  | 10,870 |
| **2f** | H | H |  | 23,910 |
| **2g** | H | H | 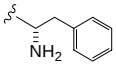 | 690 |
| **2h** | H | H | 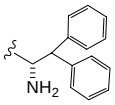 | 6760 |
| **2i** | H | H | 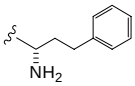 | 8020 |
| **2j** | H | H | 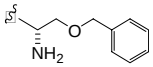 | 4040 |
| **2k** | H | H | 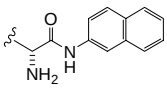 | 4%[b] |
| **2l** | H | H | 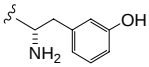 | 875 |
| **2m** | H | H | 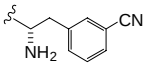 | 320 |
| **2n** | H | H | 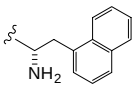 | 324 |
| **2o** | H | H | 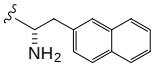 | 146 |
| **2p** | H | H | 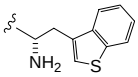 | 142 |
| **2q** | H | H | 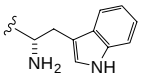 | 14 |
| **2r** | H | H | 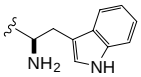 | 360 |

**Table 1** (*continued*)

| Compound | $R^1$ | $R^2$ | $R^3$ | Akt1 $IC_{50}$[a] (nM) |
|---|---|---|---|---|
| **2s** | Cl | H | 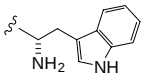 | 23 |
| **2t** | H | Cl | 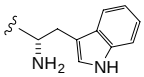 | 273 |
| **2u** | H | H | 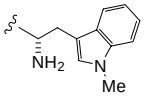 | 500 |
| **2v** | H | H | 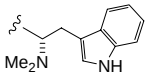 | 1100 |
| **7a** | H | H | 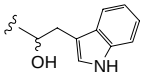 | 24,010 |
| **7b** | H | H | 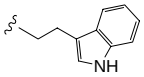 | >50,000 |

[a] Against Akt1 with ATP concentration of 10 μM.
[b] Inhibition at 5.33 μM.

with other available amino acids (Table 1).[6] Although compounds with side chains derivatized from β-alanine (**2b**), valine (**2c**), *R*-serine (**2d**), azetidine-2-carboxylic acid (**2e**), and proline (**2f**) are much less active, phenylalanine analog **2g** has an $IC_{50}$ of 690 nM, which is approximately 8-fold more potent than lead compound **1**. This result prompted us to further investigate this region of the molecule. Addition of a second phenyl group to **2g** (**2h**) or moving the phenyl ring away from the amino group (**2i** and **k**) is detrimental to the activity. On the other hand, substitution on the phenyl ring (**2l** and **m**) has little effect on the Akt1 activity, suggesting bicyclic aromatic rings might be tolerable. Indeed, the naphthyl analogs (**2n** and **o**) are 2- to 5-fold more potent than **2g**, with the 2-naphthyl compound (**2o**) being 2-fold more active than the 1-naphthyl analog (**2n**). Throughout our studies, we have found that an aromatic group in the side chain is necessary for potent Akt1 activity, with the 3-indolyl group being optimal in the current series. With an $IC_{50}$ of 14 nM, indole compound **2q** is nearly 380-fold more active than the initial lead. Note that the activities of *N*-methylindole (**2u**) and benzothiophene (**2p**) are sharply lower than that of indole **2q**. The chloro (**1**) and deschloro compounds (**2a**) have similar $IC_{50}$ values against Akt1, suggesting that the 2-chloro is not required for potency. Chloro analog **2t** is only slightly less active than **2q**.

Other side-chain modifications are summarized in Table 2. Replacing the oxygen linker with a carbon atom (**15**) resulted in a nearly 9-fold drop in activity, perhaps caused by a conformational change of the side chain. However, the nitrogen analogs (**16a** and **6c**) demonstrate a slightly better activity than the corresponding oxygen analogs **2q** and **t**. Note that reduction of the indole ring decreased activity by 4-fold (**16b**). Activity of the amides (**17a**–**d**) is markedly reduced, with tryptophan amide **17a** being the best (278 nM). Incorporation of a structure motif of HT-89, a known Akt inhibitor with an $IC_{50}$ of 2.5 μM,[1d] resulted in almost complete loss of Akt1

**Table 2.** Activity of Akt inhibitors[a]

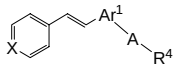


| Compound | X | $Ar^1$ | A | $R^4$ | Akt1 $IC_{50}$[b] (nM) |
|---|---|---|---|---|---|
| **15** | N | 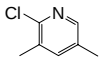 | $CH_2$ | 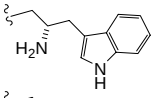 | 198 |
| **16a** | N | 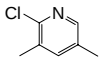 | NH | 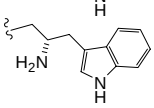 | 19 |
| **16b** | N | 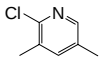 | NH | 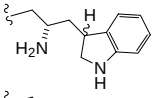 | 79 |
| **16c** | N |  | NH | 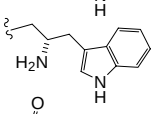 | 9.7 |
| **17a** | N |  | NH | 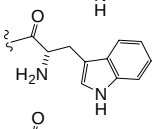 | 278 |
| **17b** | N |  | NH | 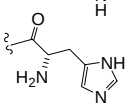 | 73%[c] |
| **17c** | N |  | NH | 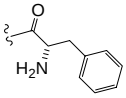 | 3200 |
| **17d** | N |  | NH | 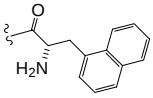 | 668 |
| **2w** | N |  | O | 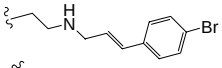 | 32,250 |
| **22a** | N |  | Bond |  | 284 |
| **22b** | N |  | Bond | 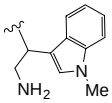 | 760 |
| **5** | CH |  | O | 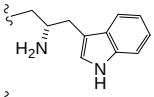 | 17%[d] |
| **6a** | N |  | O | 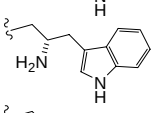 | 35%[d] |
| **6b** | N |  | O | 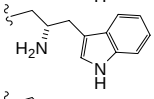 | 16%[d] |
| **6c** | N |  | O | 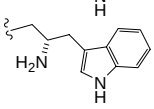 | 23,270 |
| **6d** | N |  | O | 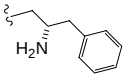 | 29%[e] |
| **6e** | N |  | O | 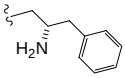 | 43,010 |

[a] Unless otherwise specified, all compounds are *S*-enantiomers.
[b] Against Akt1 with ATP concentration of 10 μM.
[c] Inhibition at 0.99 μM.
[d] Inhibition at 5.33 μM.
[e] Inhibition at 50 μM.

activity (**2w**). Compounds in which the oxygen linker is deleted (**22a** and **b**) display an unexpectedly good activity with $IC_{50}$ values slightly better than those of the corresponding oxygen analogs (**2g** and **u**).

Another salient feature of the current series is the primary amino group in the side chain. Any modification of the primary amino group, including deletion (**7b**), replacement with a hydroxy group (**7a**), and substitution with methyl groups (**2v**), resulted in a significant loss of activity. The chirality of the amino group also affects the potency, with the *S*-isomer (**2q**) exhibiting 25-fold more potency than the corresponding *R*-isomer (**2r**).

One of the most important requirements for ATP site inhibitors of Akt is having a functional group that can form hydrogen bonds with the 'hinge' region of the ATP binding pocket. The terminal pyridine in **2q** has been confirmed by X-ray structural data as the hinge-binding group.[7,8] Replacing this pyridine moiety with a phenyl group (**5**) abolishes activity (Table 2). Attempts to replace the central pyridine have not been successful. Significant loss in activity is seen for the compound with the central pyridine substituted by a phenyl group (**6a**). Additionally, the 1,3-relationship between the vinylpyridine and the side chain is critical as the *ortho*- and *para*-substituted pyridines (**6b–e**) are much less potent than the corresponding *meta*-substituted pyridines (**2g** and **q**).

Adding substituents at C-2 of the terminal pyridine in an attempt to pick up additional interactions with hinge region amino acid residues was unsuccessful (Table 3). In general, activities of the alkoxy and thioalkoxy analogs (**10a–d**) are sharply reduced. Based on X-ray crystallography, introduction of an amino group at C-2 (**10e**) was anticipated to generate an additional H-bond interaction with the hinge carbonyl group of Glu121. However, an unexpected 10-fold reduction of potency was observed. Similarly, benzyl analog **10i**, designed to interact with the nearby Phe438 of Akt1 (Phe327 in PKA),[7] displays a similar potency loss relative to parent compound **10e**.

The X-ray structure of **2q** in complex with PKA (a kinase closely related to Akt[9]) in the active site was determined (Fig. 2).[7,8] In the active site, the nitrogen of the terminal pyridine binds to the hinge via a hydrogen bond with the backbone NH of Val123. The pyridine ring is sandwiched between the isopropyl group of Leu173 underneath and the methyl group of Ala70 above, forming strong van der Waals interactions. The

**Table 3.** Activity of Akt inhibitors[a]

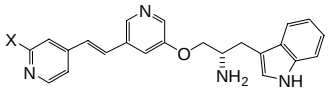


| Compound | X | $IC_{50}$[a] (nM) | Compound | X | Akt1 $IC_{50}$[a] (nM) |
|---|---|---|---|---|---|
| **10a** | MeO– | 2670 | **10f** | MeNH– | 176 |
| **10b** |  | 6450 | **10g** | EtNH– | 163 |
| **10c** |  | 6350 | **10h** |  | 69 |
| **10d** | 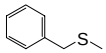 | 3110 | **10i** | 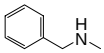 | 147 |
| **10e** | $H_2N$– | 121 | **10j** |  | 3340 |

[a] Against Akt1 with ATP concentration of 10 μM.

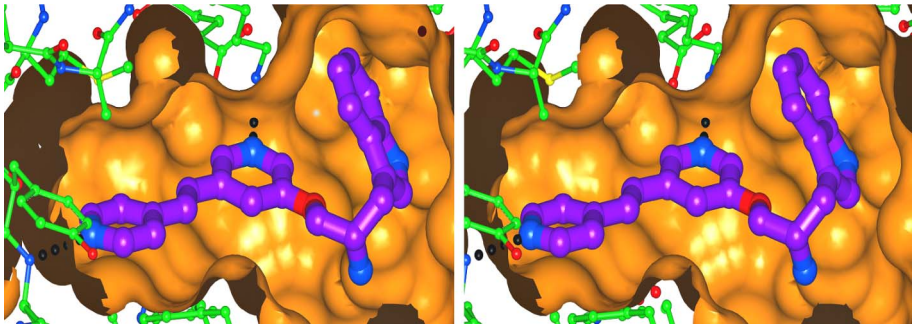

**Figure 2.** Stereoview of X-ray structure of compound **2q** in complex with PKA in the ATP binding site.

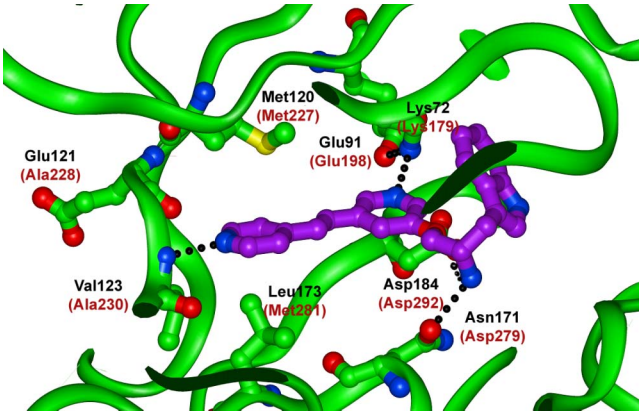


**Figure 3.** X-ray crystal structure[7] of **2q** in complex with PKA in the active site with key interactions highlighted. The amino acids highlighted in black are from PKA and red are from Akt1.

nitrogen of the central pyridine hydrogen bonds to the amino group of Lys72, which in turn forms a salt bridge with Glu91. The charged primary amine of the side chain sits tightly in the Mg-binding loop, binding to Asn171 and Asp184 via hydrogen bonds and ionic interactions. The indole ring is packed underneath the glycine-rich loop with an average distance of 3.5 Å. Interestingly, although there is no apparent interaction between the NH of the indole and the loop, *N*-methyl substitution (**2u**) is detrimental to the binding. The key interactions with PKA are highlighted in Figure 3.

With the available X-ray structure, it becomes easy to understand why substitutions at C-2 (Table 3) are detrimental. Deep inside the binding cavity, the distance between C-2 of **2q** and the carbonyl group of Glu121 is merely 3.2 Å, not enough for groups larger than hydrogen. If the C-2 hydrogen were capable of hydrogen bonding, it might be a perfect fit. Another feature of PKA and Akt is that the entrance to the ATP binding pocket near the hinge region is partially blocked by residues 315–327 (PKA) of the C-terminal domain.[2e] The nearest distance from the pyridine to Phe327 is about 3.6 Å, making it just as hard even with the amino group of **10e** facing outside of the cavity by 180° rotation of the pyridine.

Selectivity and cellular activity profiles of **2q** in comparison with those of staurosporine, a non-selective kinase inhibitor staurosporine serving as a control, are summarized in Table 4. Overall, **2q** demonstrates excellent selectivity against select families of kinases such as TK[3] and CAMK,[3] and exhibits $IC_{50}$ values of over 50 μM against most kinases. However, selectivity against closely related kinases of the AGC[3] and CMGC[3] families is marginal at best, presumably due to the high degree of homology in the ATP binding pocket. The three Akt isoforms display greater than 80% overall sequence homology and nearly 100% homology in the ATP binding pocket. In the ATP binding pocket, the non-crucial Val228 in AKT3 is the only one that is different among the three Akt isoforms. The homology between Akt1 and PKA in the ATP binding domains is low (66%), with as many as 13 different amino acids. However, none of these residues is located in the critical binding sites.[2e] These structural similarities make it difficult to achieve selectivity among these kinases.[6]

**Table 4.** Selectivity profile and cellular activity of Akt inhibitor **2q** ($IC_{50}$[a], nM)

| Test | Name | **2q** | Staurosporine |
|---|---|---|---|
| Kinases | Akt1 | 14 | 1.5 |
| | Akt2 | 257 | 6.5 |
| | Akt3 | 354 | 10 |
| | PKA | 38 | 3.6 |
| | ERK2 | 12,850 | 370 |
| | CK2 | >50,000 | 3400 |
| | Chk1 | 16,000 | 9.5 |
| | KDR | >50,000[b] | 88[b] |
| | FLT4 | >50,000[b] | 58[b] |
| | C-KIT | >50,000[b] | 23[b] |
| | SRC | >50,000[b] | 1920[b] |
| Cellular activity | GSK3-P[c,11] | 10,000 | 460 |
| | FL5.12-Akt1[10] (MTT)[d] | 3000 | 290 |
| | MiaPaCa-2 (MTT)[d] | 12,000 | 370 |

[a] Unless otherwise specified, all compounds are *S*-enantiomers, ATP concentration at 10 μM.
[b] ATP concentration at 1.0 mM.
[c] $EC_{50}$ against GSK3 phosphorylation in the Akt1 overexpressing cell FL5.12-Akt1.
[d] $IC_{50}$ against cell proliferation in MTT assays.

Compound **2q** was evaluated for its antiproliferative activity against FL5.12-Akt1 murine prolymphocytic cells[10] that overexpress Akt1 and MiaPaCa-2 human pancreatic cancer cells. Compound **2q** displays $IC_{50}$ values of 3.0 and 12.0 μM against FL5.12-Akt1 and MiaPaCa-2, respectively. Compound **2q** also inhibits the phosphorylation of the Akt downstream target GSK3[11] in FL5.12-Akt1 cells with an $EC_{50}$ of 10.0 μM. Apparently, staurosporine is more potent than **2q** in these tests.

Pharmacokinetic (PK) properties of selected Akt inhibitors are summarized in Table 5. Overall, compounds with an oxygen linker (**2p**,**q**, and **s**) show favorable oral bioavailability. Compounds **2q** and **s**, which differ only by a chlorine atom, share similar PK profiles in four different species with oral bioavailabilities ranging from 11% to 52%. In rat, **2p** displays an oral bioavailability of 43%, which is 2-fold better than that of **2q**, suggesting that the indole in **2q** is an unfavorable group for PK. The compounds with either a carbon (**15**) or a nitrogen linker (**16a**) demonstrate extremely high clearance in mouse resulting in poor overall PK.

In summary, a novel series of inhibitors of PKB/Akt derived from a screening lead (**1**) has been prepared. The novel series of 3,4′-bispyridinylethylenes as represented by **2q** are potent Akt inhibitors with $IC_{50}$ values in the low double-digit nanomolar rang against Akt1. Compound **2q** shows excellent selectivity against distinct families of kinases such as TK and CAMK, and displays poor to marginal selectivity against the AGC and

**Table 5.** Pharmacokinetic properties of selected Akt inhibitors[12]

| Compound | Species | $t_{1/2}$ (h) | $V_\beta$ (L/kg) | $Cl_p$ (L/h kg) | $C_{max}$ (μg/mL) | AUC (oral) | Oral F (%) |
|---|---|---|---|---|---|---|---|
| **2p** | Rat[a] | 2.5 | 3.6 | 1.0 | 0.62 | 2.13 | 43 |
| **2q** | Mouse[b] | 0.8 | 6.5 | 5.7 | 2.78 | 5.5 | 39 |
| | Rat[a] | 3.1 | 5.2 | 1.2 | 0.30 | 0.95 | 21 |
| | Dog[c] | 3.2 | 12.8 | 2.5 | 0.10 | 0.50 | 52 |
| | Monkey[c] | 3.7 | 9.1 | 1.6 | 0.04 | 0.19 | 12 |
| **2s** | Mouse[b] | 0.8 | 4.8 | 4.1 | 0.94 | 1.45 | 11 |
| | Rat[a] | 3.1 | 9.9 | 2.2 | 0.06 | 0.38 | 17 |
| | Dog[c] | 5.4 | 11.1 | 1.4 | 0.12 | 1.01 | 45 |
| | Monkey[c] | 3.0 | 4.2 | 0.97 | 0.06 | 0.30 | 12 |
| **15** | Mouse[d] | 0.2 | 4.9 | 17.3 | 0.09 | <0.1 | <10 |
| **16a** | Mouse[d] | 0.6 | 9.5 | 11.4 | <0.02 | 0 | 0 |

[a] A single 5 mg/kg dose.
[b] A single 30 mg/kg dose.
[c] A single 2.5 mg/kg dose.
[d] A single 10 mg/kg dose.

CMGC families of kinases.[3] Compound **2q** also demonstrates moderate antiproliferative activity against FL5.12-Akt1 and MiaPaCa-2 cells. Inhibition of phosphorylation of the downstream target GSK3 is observed for **2q**. Moreover, the current series have respectable oral bioavailabilities across four different animal species. These encouraging preliminary results warrant further efforts to optimize the physiochemical and biological properties of this series.

## Acknowledgments

The authors are grateful to Mr. Rick Clark, Dr. Moshe Weitzberg, Dr. Matt. Hensen, Dr. Robert Keyes, Dr. Curt Cooper, and Dr. Chris Krueger for proofreading and suggestions. X-ray crystallographic data were collected at beamline 17-ID in the facilities of the Industrial Macromolecular Crystallography Association Collaborative Access Team (IMCA-CAT) at the Advanced Photon Source, which are supported by the companies of the Industrial Macromolecular Crystallography Association.

## References and notes

1. (a) Zhao, Z.; Leister, W. H.; Robinson, R. G.; Barnett, S. F.; Defeo-Jones, D.; Jones, R. E.; Hartman, G. D.; Huff, J. R.; Huber, H. E.; Duggan, M. E.; Lindsley, C. W. *Bioorg. Med. Chem. Lett.* **2005**, *15*, 905; (b) Lindsley, C. W.; Zhao, Z.; Leister, W. H.; Robinson, R. G.; Barnett, S. F.; Defeo-Jones, D.; Jones, R. E.; Hartman, G. D.; Huff, H. E.; Duggan, M. E. *Bioorg. Med. Chem. Lett.* **2005**, *15*, 761; (c) Breitenlechner, C. B.; Wegge, T.; Berillon, L.; Graul, K.; Marzenell, K.; Friebe, W.-G.; Thomas, U.; Schumacher, R.; Huber, R.; Engh, R. A.; Masjost, B. *J. Med. Chem.* **2004**, *47*, 1375; (d) Reuveni, H.; Livnah, N.; Geiger, T.; Klein, S.; Ohne, O.; Cohen, I.; Benhar, M.; Gellerman, G.; Levitzki, A. *Biochemistry* **2002**, *41*, 10304.
2. For recent reviews on Akt, see: (a) Barnett, F. S.; Bilodeau, M. T.; Lindsley, C. W. *Curr. Top. Med. Chem.* **2005**, *5*, 109; (b) Mitsiades, C. S.; Mitsiades, N.; Koutsilieris, M. *Curr. Cancer Drug Targets* **2004**, *4*, 235; (c) Gills, J. J.; Dennis, P. A. *Expert Opin. Invest. Drugs* **2004**, *13*, 787; (d) Vivanco, I.; Sawyers, C. L. *Nat. Rev. Cancer* **2002**, *2*, 489; (e) Li, Q.; Zhu, G.-D. *Curr. Top. Med. Chem.* **2002**, *2*, 939.
3. Hanks, S.; Hunter, T. *FASEB J.* **1995**, *9*, 576.
4. Cheng, J. Q.; Ruggeri, B.; Klein, W. M.; Sonoda, G.; Altomare, D. A.; Watson, D. K.; Testa, J. R. *Proc. Natl. Acad. Sci. U.S.A.* **1996**, *93*, 3636.
5. Rocca, P.; Cochennec, C.; Marsais, F.; Thomas-dit-Dument, L.; Mallet, M.; Godard, A.; Queguiner, G. *J. Org. Chem.* **1993**, *58*, 7832.
6. Luo, Y.; Shoemaker, A.; Liu, X.; Woods, K.; Thomas, S.; de Jong, R.; Han, E.; Li, T.; Stoll, S. S.; Powelas, J. A.; Oleksijew, A.; Mitten, M. J.; Shi, Y.; Guan, R.; McGonigal, T. P.; Klinghofer, V.; Johnson, E. F.; Leverson, J. D.; Bouska, J. J.; Mamo, M.; Smith, R. A.; Gramling-Evans, E. E.; Zinker, B. A.; Mika, A. K.; Nguyen, P. T.; Oltersdorf, T.; Rosenberg, S. H.; Li, Q.; Giranda, V. *Mol. Cancer Ther.* **2005**, *4*, 977.
7. PKA and **2q** were co-crystallized in a solution containing PKA (20 mg/mL) and PKI peptide according to a method of Engh et al.[8] The structure was determined and refined to resolutions of 1.9 Å ($R_{work}$ = 30.92% and $R_{Free}$ = 33.78%). The crystallographic data have been deposited with PDB (ID: 2F7X).
8. Engh, R. A.; Girod, A.; Kinzel, V.; Huber, R.; Bossemeyer, D. *J. Biol. Chem.* **1996**, *271*, 26157.
9. Hanada, M.; Feng, J.; Hemmings, B. A. *Biochim. Biophys. Acta* **2004**, *1697*, 3.
10. Plas, D. R.; Talapatra, S.; Edinger, A. L.; Rathmell, J. C.; Thompson, C, B. *J. Biol. Chem.* **2001**, *276*, 12041.
11. Liu, X.; Powlas, J.; Shi, Y.; Oleksijew, A. X.; Shoemaker, A. R.; de Jong, R.; Oltersdorf, T.; Giranda, V. L.; Luo, Y. *Anticaner Res.* **2004**, *5A*, 2697.
12. Pharmacokinetic properties were determined by traditional single-dose methods with plasma concentrations determined by HPLC–MS as described previously: Li, Q.; Woods, K. W.; Claiborne, A.; Gwaltney, S. L., II; McCroskey, R. W.; Barr, K. J.; McCroskey, R. W.; Wang, L.; Szczepankiewicz, B. G.; Liu, G.; Gehrke, L.; Credo, R. B.; Hui, Y. H.; Marsh, K.; Warner, R. B.; Lee, J. Y.; Zielinski, N. A.; Frost, D.; Ng, S. C.; Rosenberg, S. H.; Sham, H. *Bioorg. Med. Chem. Lett.* **2002**, *12*, 465.